Observations and Analysis of the Extreme Mass Ratio, High Fill-out Solar Type Binary, V1695 Aquilae

Ronald G. Samec
Christopher R. Gray
Natural Sciences Department, Emmanuel College,181 Springs Street, Franklin Springs, GA 30639; ronaldsamec@gmail.com

Daniel Caton
Dark Sky Observatory, Department of Physics and Astronomy, Appalachian State University, 525 Rivers Street, Boone, NC 28608

Danny R. Faulkner
Johnson Observatory, 1414 Bur Oak Court, Hebron, KY 41048

Robert Hill
Department of Chemistry and Physics, Bob Jones University, 1700 Wade Hampton Boulevard, Greenville, SC 29614

Walter Van Hamme
Department of Physics, Florida International University,11200 SW 8th Street, CP 204, Miami, FL 33199

Received June 28, 2017; revised August 8, 2017; accepted August 14, 2017

Abstract CCD BVR$_c$I$_c$ light curves of V1695 Aquilae were taken during the Fall 2016 season at the Cerro Tololo InterAmerican Observatory with the 0.6-meter reflector of the SARA South observatory in remote mode. It is an eclipsing binary with a period of 0.41283 d. The light curves yield a total eclipse (duration: 59 minutes) but have an amplitude of only ~0.4 mag. The spectral type is ~G8V (~5500 K). Four times of minimum light were calculated, all primary eclipses, from our present observations. We calculated linear and quadratic ephemerides from all available times of minimum light. A 17-year period study reveals a quadratic orbital period decrease at a high level of confidence. The orbital period is changing at a rapid rate of of $dp/dt = -1.73 \times 10^{-6}$ d/yr. The solution is that of an Extreme Mass Ratio Binary. The mass ratio is found to be near 0.16. Its Roche Lobe fill-out is a hefty 83%. The small component has the slightly hotter temperature of ~5650 K, which makes it a W-type W UMa Binary. As expected in binaries of this spectral type, it has cool spot regions.

1. Introduction

In this study of V1695 Aql, our analysis includes its observation, a period study, and light curve analysis of an extreme mass ratio solar type Southern eclipsing binary. We used the Wilson-Devinney Program (WD; Wilson and Devinney 1971) for this calculation. This paper represents the first published BVRcIc light curves and analysis of V1695 Aql. Observers prize total eclipsing contact binaries since they give unambiguous solutions with mass ratios even without difficult-to-obtain precision radial velocity curves. These require large telescopes (we estimate a 3.5 to 4-meter telescope is needed for this variable). Many forget about velocity smearing with such a system which requires a higher signal-to-noise.

Contact binaries are numerous in number and represent a challenge to present-day stellar theory. It is believed that (for those of solar type), that they begin their existence as well detached fast spinning stars in groups that undergo gravitational interactions which leave them as binaries with several-day periods. Since they are highly magnetic in nature, due to their convective envelopes and fast rotation, they undergo magnetic braking as plasma winds leave the stars on stiff rotating dipole fields. This action torques the binary, eventually bringing them into contact and finally leaving a single, fast rotating star.

2. History and observations

V1695 Aql (GSC 5149 2845) was discovered as part of an initiative to classify variable stars using CCD observations by Bernhard *et al.* (2002). The star was typed as a W UMa binary with a V magnitude ≈11.0. Their light curve is shown as Figure 1.

Their ephemeris is:

$$\text{MinI} = \text{HJD } 2452522.440 \pm 0.007 + 0.4128 \pm 0.0001 \text{ d} \times E \quad (1)$$

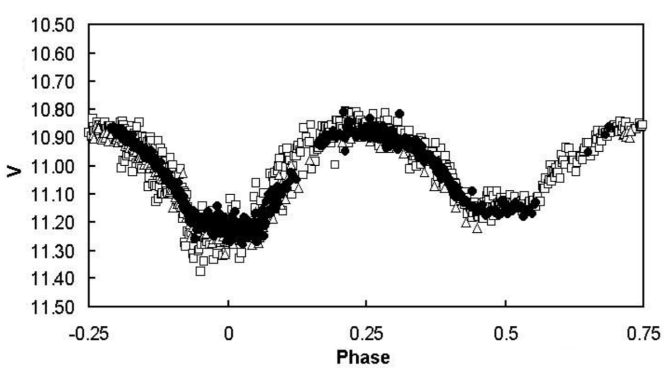

Figure 1. Light curve of V1695 Aql by Bernhard *et al.* 2002.

Kreiner (2004) gives the following:

$$\text{MinI} = \text{HJD } 2456102.460 + 0.4127768 \text{ d} \times \text{E} \qquad (2)$$

A number of eclipse timings are given by Pejcha (2005), Berhard *et al.* (2002), and Paschke (1994, 2002).

V1695 Aql is likely an x-ray source (1RXSJ193821.2-033245), which is not unusual for active W UMa variables (Szczygiel *et al.* 2008). It is included in the Automated Variable Star classification (ID 14143847) via the NSVS (Hoffman *et al.* 2009) and is listed in the 78th name list (Kazarovets *et al.* 2006). The observations were undertaken by Samec, Gray, Faulkner, Hill, and Van Hamme. Reduction and analyses were done by Samec and Gray.

3. Photometry

Our photometry was taken with the Southeastern Association for Research in Astronomy (SARA South) Telescope at Cerro Tololo InterAmerican Observatory (CTIO) in remote mode. The 24-inch f/11 Boller and Chivens reflector was used on four nights, 14 August and 3–5 September, 2016, with the ARC Camera cooled to –60° C. We used standard BVR_cI_c Johnson-Cousins filters. The precision of a single observation was good, 0.010 in B, V, I_c, and 0.014 in R_c. The observations included 185 in B, 187 in V, 162 in R_c, and 187 in I_c. Exposure times varied from 250–275 seconds in B, 80–90 seconds in V, and 30–50 seconds in R_c and I_c. Nightly images were calibrated with 25 bias frames, at least five flat frames in each filter, and ten 300-second dark frames. Figure 2a and 2b show sample observations of B, V, and B–V color curves on the night of August 14 and September 23, 2016. Our observations are given in Table 1, in delta magnitudes, ΔB, ΔV, ΔR_c, and ΔI_c, in the sense of variable minus comparison star.

4. Finding chart

The finding chart is shown as Figure 3. The coordinates and magnitudes of the variable star, comparison star, and check star are given in Table 2. Our B–V and R_c–I_c Comparison-Variable magnitude curves show that the variable and comparison stars are near spectral matches with Δ(B–V) and Δ (R–I) ≈ 0. The nightly C–K values stayed constant throughout the observing run with a precision of $\approx 1\%$.

5. Period study

Four times of minimum light were calculated from our present observations, all primary eclipses, using the method of Kwee and Van Woerden (1956) performed by Caton:

$$\begin{aligned} \text{HJD} = {} & 2457614.68359 \pm 0.0002 \text{ d} \\ & 2457634.49320 \pm 0.00037 \text{ d} \\ & 2457636.56250 \pm 0.00006 \text{ d} \\ & 2457635.68247 \pm 0.00002 \text{ d} \end{aligned}$$

Additional timings were gathered from other sources using the O–C gateway (http://var2.astro.cz/ocgate/) and the Nelson Database of Times of Minima (Nelson 2016). These included Berhard *et al.* (2002), and Pejcha (2005). We note that our last timing was removed from our analysis due to its large residual. The following linear and quadratic ephemerides were determined from all available times of minimum light:

$$\text{JD Hel MinI} = 2452576.3106 \pm 0.0060 \text{ d} + 0.41282964 \pm 0.00000080 \times \text{E} \qquad (2)$$

$$\text{JD Hel MinI} = 2452576.3191 \pm 0.0024 \text{ d} + 0.4128401 \pm 0.0000011 \times \text{E} - 9.75 \pm 1.0 \times 10^{-10} \times \text{E}^2 \qquad (3)$$

The O–C residuals for both linear and quadratic calculations are given in Table 3. Thus, the 17-year period study reveals that the system is undergoing a smooth quadratic decrease in orbital period. The changing period would be expected for the process of magnetic braking (e.g., Gazeas and Stępień 2008). The value of the rate of change in the orbital period is $dp/dt = -1.73 \times 10^{-6}$ d/yr. Third body interactions and normal stellar evolution may play a role, but a much longer interval of observation is needed to determine if this is the case. A plot of the quadratic term overlying the linear residuals of Equation 3 is shown in Figure 4.

6. Light curve characteristics

The light curves of V1695 Aql phased using Equation 2, delta mag vs. phase, are shown in Figure 5a and 5b. Light curve amplitudes and the differences in magnitudes at various quadratures are given in Table 4. The primary amplitudes of the light curves are about 0.4 magnitude in all filters while the secondary's are ~ 0.3 magnitude. This points to a rather large difference in minima, 0.07–0.08 magnitude, for an over contact binary. These values are usually thought of as indicators of the degree of thermal contact. In this case, it may be an indicator of large spot regions. In general, the asymmetries throughout the light curve point to the presence of spot activity. This is apparent when we compare the early curve (Figure 1) to our present ones. In Figure 6, a plot of the night to night variability in the light curves in B and V is given. This shows that the magnetic activity causes rapid changes in the light curves. The light curves are distinctly over contact. The low amplitudes indicate that the binary has a very small mass ratio so the binary belongs to the family of extreme-mass ratio binaries. To extend this analysis we undertook a Wilson-Devinney program light curve solution. The light curves yielded a very long eclipse duration of 59 minutes for a binary, with a period of 9.9 hours as determined from this solution.

7. Temperature and light curve solution

BINARY MAKER 3.0 (Bradstreet and Steelman 2002) was used to explore the character of our light curves and determine initial parameters of each of the B, V, Rc, Ic light curves. The Wilson-Deviney program requires a fairly good fitting curve to begin the process, however the final solution parameters may have little resemblance to the initial values. For instance, our B-filter light curve gave a mass-ratio of 0.15 using BINARY

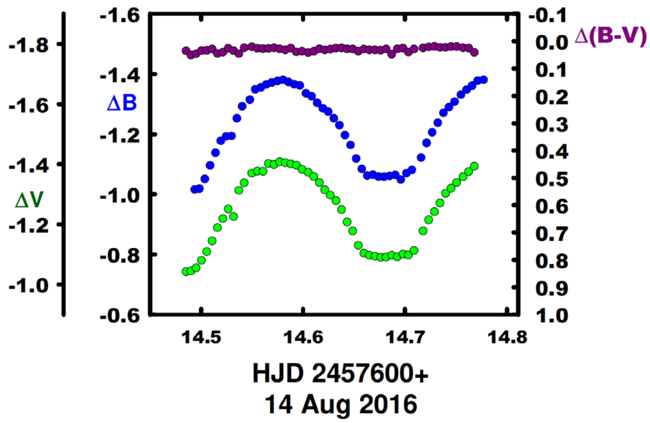

Figure 2a. B, V, and B–V color curves of V1695 Aql on the night of August 14, 2016.

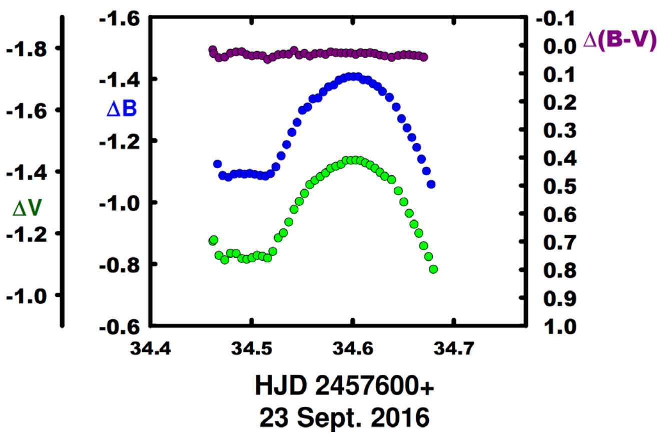

Figure 2b. B, V, and B–V color curves of V1695 Aql on the night of September 23, 2016.

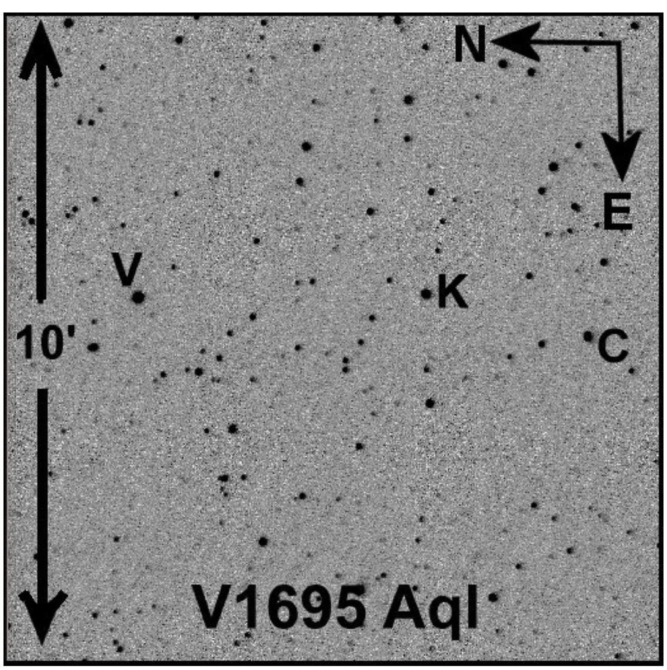

Figure 3. Finding Chart of V1695 Aql including Variable (V), Comparison (C), and Check Stars (K).

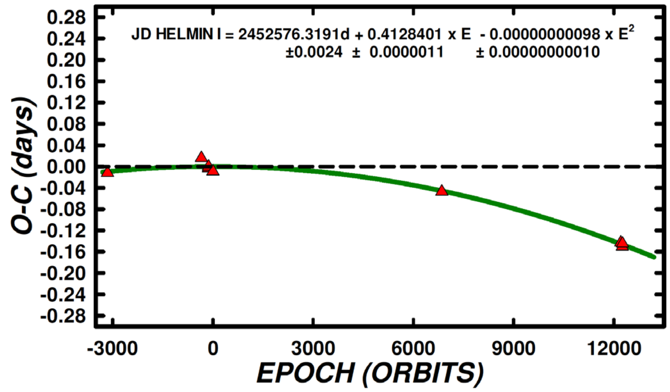

Figure 4. O–C residuals from the quadratic ephemeris of V1695 Aql from Equation 3.

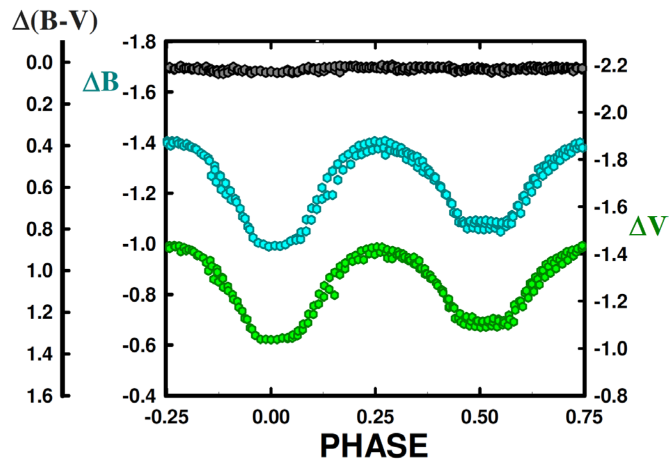

Figure 5a. B, V delta magnitudes of V1695 Aql, phased using Equation 2.

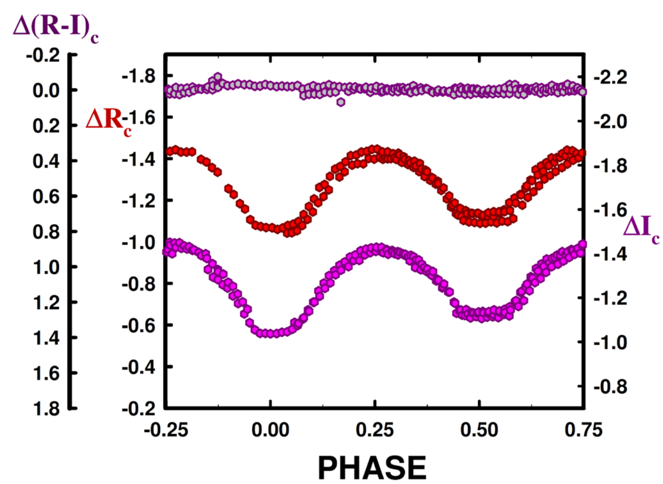

Figure 5b. R_c, I_c delta magnitudes of V1695 Aql, phased using Equation 2.

Table 1. V1695 Aql observations, ΔB, ΔV, ΔR_c, and ΔI_c, variable star minus comparison star.

ΔB	HJD 2457600+	ΔB	HJD 2457600+	ΔB	HJD 2457600+	ΔB	HJD 2457600+	ΔB	HJD 2457600+
–1.042	14.4856	–1.093	14.6709	–1.258	34.538	–1.415	35.604	–1.138	36.549
–1.044	14.4903	–1.089	14.676	–1.297	34.543	–1.418	35.609	–1.137	36.554
–1.054	14.4954	–1.090	14.682	–1.347	34.548	–1.432	35.615	–1.121	36.560
–1.079	14.5006	–1.096	14.687	–1.365	34.553	–1.435	35.620	–1.123	36.565
–1.108	14.5058	–1.091	14.693	–1.381	34.559	–1.445	35.625	–1.123	36.571
–1.144	14.5111	–1.100	14.698	–1.404	34.564	–1.446	35.630	–1.145	36.576
–1.188	14.5163	–1.097	14.704	–1.405	34.569	–1.433	35.635	–1.145	36.582
–1.218	14.5216	–1.112	14.709	–1.424	34.574	–1.433	35.640	–1.151	36.587
–1.250	14.5268	–1.177	14.718	–1.441	34.579	–1.424	35.646	–1.187	36.593
–1.312	14.5373	–1.214	14.724	–1.438	34.585	–1.427	35.651	–1.226	36.598
–1.337	14.5425	–1.241	14.729	–1.256	35.483	–1.410	35.656	–1.269	36.604
–1.369	14.5500	–1.270	14.735	–1.228	35.488	–1.391	35.661	–1.294	36.609
–1.376	14.5554	–1.302	14.740	–1.184	35.494	–1.388	35.667	–1.322	36.614
–1.375	14.5609	–1.319	14.746	–1.158	35.499	–1.377	35.672	–1.339	36.620
–1.401	14.5663	–1.338	14.751	–1.107	35.505	–1.345	35.678	–1.367	36.625
–1.398	14.5718	–1.357	14.757	–1.080	35.510	–1.310	35.684	–1.382	36.631
–1.407	14.5773	–1.374	14.763	–1.074	35.515	–1.292	35.690	–1.406	36.636
–1.404	14.5828	–1.392	14.768	–1.069	35.520	–1.397	36.461	–1.413	36.642
–1.400	14.5882	–1.404	14.774	–1.068	35.526	–1.399	36.466	–1.416	36.647
–1.396	14.5937	–1.168	34.465	–1.060	35.531	–1.404	36.473	–1.425	36.653
–1.382	14.5992	–1.137	34.469	–1.067	35.537	–1.418	36.478	–1.427	36.658
–1.372	14.6052	–1.123	34.475	–1.079	35.542	–1.397	36.483	–1.435	36.664
–1.358	14.6107	–1.137	34.480	–1.085	35.547	–1.379	36.489	–1.443	36.669
–1.338	14.6162	–1.137	34.486	–1.098	35.552	–1.365	36.494	–1.432	36.675
–1.314	14.6216	–1.138	34.491	–1.132	35.557	–1.351	36.500	–1.432	36.680
–1.296	14.6271	–1.127	34.496	–1.170	35.563	–1.338	36.505	–1.433	36.686
–1.278	14.6326	–1.140	34.501	–1.207	35.568	–1.308	36.510	–1.397	36.694
–1.248	14.6381	–1.145	34.507	–1.262	35.573	–1.281	36.516	–1.384	36.700
–1.207	14.6435	–1.136	34.512	–1.276	35.578	–1.259	36.521	–1.357	36.705
–1.177	14.6490	–1.154	34.517	–1.315	35.583	–1.221	36.527	–1.335	36.711
–1.129	14.6545	–1.188	34.522	–1.350	35.588	–1.187	36.532		
–1.103	14.6600	–1.211	34.527	–1.363	35.594	–1.161	36.538		
–1.096	14.6654	–1.228	34.533	–1.385	35.599	–1.150	36.543		

ΔV	HJD 2457600+	ΔV	HJD 2457600+	ΔV	HJD 2457600+	ΔV	HJD 2457600+	ΔV	HJD 2457600+
–1.088	14.493	–1.284	14.634	–1.418	14.781	–1.423	34.590	–1.337	35.677
–1.084	14.497	–1.249	14.640	–1.407	14.779	–1.443	34.595	–1.319	36.511
–1.110	14.502	–1.226	14.645	–1.399	14.785	–1.057	35.546	–1.280	36.516
–1.139	14.507	–1.180	14.651	–1.130	34.470	–1.074	35.551	–1.262	36.522
–1.180	14.513	–1.141	14.656	–1.121	34.476	–1.103	35.557	–1.226	36.527
–1.207	14.518	–1.120	14.662	–1.127	34.481	–1.145	35.562	–1.175	36.533
–1.243	14.523	–1.109	14.667	–1.131	34.487	–1.231	35.572	–1.145	36.538
–1.267	14.528	–1.115	14.673	–1.136	34.492	–1.266	35.577	–1.146	36.544
–1.304	14.534	–1.106	14.678	–1.132	34.497	–1.300	35.582	–1.133	36.549
–1.325	14.539	–1.112	14.683	–1.137	34.502	–1.322	35.588	–1.131	36.555
–1.341	14.546	–1.114	14.689	–1.145	34.507	–1.347	35.593	–1.138	36.560
–1.368	14.552	–1.110	14.694	–1.136	34.512	–1.362	35.598	–1.129	36.566
–1.369	14.557	–1.124	14.700	–1.147	34.517	–1.384	35.603	–1.124	36.571
–1.394	14.562	–1.118	14.705	–1.159	34.523	–1.394	35.608	–1.140	36.577
–1.404	14.568	–1.161	14.714	–1.182	34.528	–1.413	35.614	–1.133	36.582
–1.410	14.573	–1.187	14.720	–1.224	34.533	–1.420	35.619	–1.145	36.588
–1.408	14.579	–1.232	14.725	–1.250	34.538	–1.426	35.624	–1.187	36.593
–1.415	14.584	–1.269	14.731	–1.295	34.543	–1.429	35.629	–1.229	36.598
–1.406	14.590	–1.287	14.736	–1.332	34.549	–1.428	35.634	–1.262	36.604
–1.394	14.595	–1.315	14.742	–1.353	34.554	–1.418	35.640	–1.289	36.609
–1.394	14.601	–1.341	14.747	–1.375	34.559	–1.414	35.645	–1.321	36.615
–1.367	14.607	–1.352	14.753	–1.378	34.564	–1.408	35.650	–1.342	36.620
–1.337	14.612	–1.366	14.759	–1.393	34.569	–1.399	35.655	–1.358	36.626
–1.327	14.618	–1.382	14.764	–1.408	34.575	–1.384	35.661	–1.383	36.631
–1.320	14.623	–1.396	14.770	–1.408	34.580	–1.386	35.666	–1.392	36.637
–1.301	14.629	–1.402	14.776	–1.415	34.585	–1.371	35.671	–1.396	36.642

Table continued on following pages

Table 1. V1695 Aql observations, ΔB, ΔV, ΔR_c, and ΔI_c, variable star minus comparison star, cont.

ΔR_c	HJD 2457600+	ΔR_c	HJD 2457600+	ΔR_c	HJD 2457600+	ΔR_c	HJD 2457600+	ΔR_c	HJD 2457600+
–1.042	14.486	–1.093	14.671	–1.258	34.538	–1.415	35.604	–1.138	36.549
–1.044	14.490	–1.089	14.676	–1.297	34.543	–1.418	35.609	–1.137	36.554
–1.054	14.495	–1.090	14.682	–1.347	34.548	–1.432	35.615	–1.121	36.560
–1.079	14.501	–1.096	14.687	–1.365	34.553	–1.435	35.620	–1.123	36.565
–1.108	14.506	–1.091	14.693	–1.381	34.559	–1.445	35.625	–1.123	36.571
–1.144	14.511	–1.100	14.698	–1.404	34.564	–1.446	35.630	–1.145	36.576
–1.188	14.516	–1.097	14.704	–1.405	34.569	–1.433	35.635	–1.145	36.582
–1.218	14.522	–1.112	14.709	–1.424	34.574	–1.433	35.640	–1.151	36.587
–1.250	14.527	–1.177	14.718	–1.441	34.579	–1.424	35.646	–1.187	36.593
–1.312	14.537	–1.214	14.724	–1.438	34.585	–1.427	35.651	–1.226	36.598
–1.337	14.543	–1.241	14.729	–1.256	35.483	–1.410	35.656	–1.269	36.604
–1.369	14.550	–1.270	14.735	–1.228	35.488	–1.391	35.661	–1.294	36.609
–1.376	14.555	–1.302	14.740	–1.184	35.494	–1.388	35.667	–1.322	36.614
–1.375	14.561	–1.319	14.746	–1.158	35.499	–1.377	35.672	–1.339	36.620
–1.401	14.566	–1.338	14.751	–1.107	35.505	–1.345	35.678	–1.367	36.625
–1.398	14.572	–1.357	14.757	–1.080	35.510	–1.310	35.684	–1.382	36.631
–1.407	14.577	–1.374	14.763	–1.074	35.515	–1.292	35.690	–1.406	36.636
–1.404	14.583	–1.392	14.768	–1.069	35.520	–1.397	36.461	–1.413	36.642
–1.400	14.588	–1.404	14.774	–1.068	35.526	–1.399	36.466	–1.416	36.647
–1.396	14.594	–1.168	34.465	–1.060	35.531	–1.404	36.473	–1.425	36.653
–1.382	14.599	–1.137	34.469	–1.067	35.537	–1.418	36.478	–1.427	36.658
–1.372	14.605	–1.123	34.475	–1.079	35.542	–1.397	36.483	–1.435	36.664
–1.358	14.611	–1.137	34.480	–1.085	35.547	–1.379	36.489	–1.443	36.669
–1.338	14.616	–1.137	34.486	–1.098	35.552	–1.365	36.494	–1.432	36.675
–1.314	14.622	–1.138	34.491	–1.132	35.557	–1.351	36.500	–1.432	36.680
–1.296	14.627	–1.127	34.496	–1.170	35.563	–1.338	36.505	–1.433	36.686
–1.278	14.633	–1.140	34.501	–1.207	35.568	–1.308	36.510	–1.397	36.694
–1.248	14.638	–1.145	34.507	–1.262	35.573	–1.281	36.516	–1.384	36.700
–1.207	14.644	–1.136	34.512	–1.276	35.578	–1.259	36.521	–1.357	36.705
–1.177	14.649	–1.154	34.517	–1.315	35.583	–1.221	36.527	–1.335	36.711
–1.129	14.655	–1.188	34.522	–1.350	35.588	–1.187	36.532		
–1.103	14.660	–1.211	34.527	–1.363	35.594	–1.161	36.538		
–1.096	14.665	–1.228	34.533	–1.385	35.599	–1.150	36.543		

Table continued on next page

MAKER and fill-out of 0.25. We modeled two cool spots and one hot spot to fit the asymmetries. The hot spot vanished as the Wilson program progressed. Tycho and 2MASS photometry indicated that the spectral type fell in the G6 to G9 range so a temperature of 5500 K was chosen for the primary component with the secondary component modeling at a somewhat higher temperature. Next, the mean values from the BINARY MAKER fits a set of starting values for the WD program (Wilson and Devinney 1971; Wilson 1990, 1994, 2001, 2004; Van Hamme and Wilson 1998, 2003). This version includes Kurucz atmospheres, rather than black body, and a detailed reflection treatment along with two-dimentional limb-darkening coefficients. The differential corrections routine was iterated until convergence was achieved for a solution. The solution was computed in Mode 3, the contact binary mode. Convective parameters g = 0.32, A = 0.5 were used. The light curve solution is given in Table 5.

The normalized curves overlain by our light curve solutions are shown as Figure 7a and 7b. A geometrical (Roche-lobe) representation of the system is given in Figure 8 (a, b, c, d) at light curve quadratures so that the reader may see the placement of the spots and the relative size of the stars as compared to the orbit. Table 6 gives the unspotted solution for V1695 Aql. One can compare the WD program's sum of square residual, 0.19 vs. 0.15, for the unspotted vs. the spotted model. The spotted solution presents a better numerical solution. It is noted that the unspotted solution has a somewhat smaller fill-out, 35%.

8. Conclusion

V1695 Aql is a moderate period (P = 0.4128296 day), W UMa eclipsing binary. The 17-year orbital study (more than 15,000 orbits) reveals a quadratically decreasing ephemeris. Given that the temperature for the primary component is ~5500 K, from T_2 we find the secondary (smaller) star is at a hotter ~5650 K. This effect is believed to be due to the actual saturated spot coverage on the primary component. The WD program solution gives a mass ratio of 0.16. Rasio (1995) stated the runaway event that results in a merger happens when the mass ratio is ~ 0.09, so we are 0.07 away from that event if this is the case. The Roche Lobe fill-out is rather large, 83% for this contact binary. This value could lead the system into an instability which could result in coalescence.

Recently, Molnar *et al.* (2017) predicted that the eclipsing binary KIC 9832227 would become a red nova in the year 2022. Table 7 shows a comparison of the parameters for KIC 9832227 with V1695 Aql to show the similarity of the two systems. Molnar (2017) has examined our period study curves and does not see the expected asymmetry (right side of the curve should

Table 1. V1695 Aql observations, ΔB, ΔV, ΔR_c, and ΔI_c, variable star minus comparison star, cont.

ΔI_c	HJD 2457600+	ΔI_c	HJD 2457600+	ΔI_c	HJD 2457600+	ΔI_c	HJD 2457600+	ΔI_c	HJD 2457600+
–1.088	14.493	–1.124	14.700	–1.408	34.580	–1.103	35.557	–1.262	36.522
–1.084	14.497	–1.118	14.705	–1.415	34.585	–1.145	35.562	–1.226	36.527
–1.110	14.502	–1.161	14.714	–1.423	34.590	–1.180	35.567	–1.175	36.533
–1.139	14.507	–1.187	14.720	–1.443	34.595	–1.231	35.572	–1.145	36.538
–1.180	14.513	–1.232	14.725	–1.451	34.599	–1.266	35.577	–1.146	36.544
–1.207	14.518	–1.269	14.731	–1.448	34.604	–1.300	35.582	–1.133	36.549
–1.243	14.523	–1.287	14.736	–1.449	34.609	–1.322	35.588	–1.131	36.555
–1.267	14.528	–1.315	14.742	–1.435	34.614	–1.347	35.593	–1.138	36.560
–1.304	14.534	–1.341	14.747	–1.431	34.618	–1.362	35.598	–1.129	36.566
–1.325	14.539	–1.352	14.753	–1.417	34.623	–1.384	35.603	–1.124	36.571
–1.341	14.546	–1.366	14.759	–1.405	34.628	–1.394	35.608	–1.140	36.577
–1.368	14.552	–1.382	14.764	–1.399	34.635	–1.413	35.614	–1.133	36.582
–1.369	14.557	–1.396	14.770	–1.354	34.641	–1.420	35.619	–1.145	36.588
–1.394	14.562	–1.402	14.776	–1.327	34.647	–1.426	35.624	–1.187	36.593
–1.404	14.568	–1.418	14.781	–1.307	34.652	–1.429	35.629	–1.229	36.598
–1.410	14.573	–1.407	14.779	–1.270	34.657	–1.428	35.634	–1.262	36.604
–1.408	14.579	–1.399	14.785	–1.252	34.662	–1.418	35.640	–1.289	36.609
–1.415	14.584	–1.130	34.470	–1.217	34.667	–1.414	35.645	–1.321	36.615
–1.406	14.590	–1.121	34.476	–1.181	34.671	–1.408	35.650	–1.342	36.620
–1.394	14.595	–1.127	34.481	–1.148	34.676	–1.399	35.655	–1.358	36.626
–1.394	14.601	–1.131	34.487	–1.328	35.463	–1.384	35.661	–1.383	36.631
–1.367	14.607	–1.136	34.492	–1.293	35.468	–1.386	35.666	–1.392	36.637
–1.337	14.612	–1.132	34.497	–1.282	35.473	–1.371	35.671	–1.396	36.642
–1.327	14.618	–1.137	34.502	–1.259	35.477	–1.337	35.677	–1.418	36.648
–1.320	14.623	–1.145	34.507	–1.244	35.482	–1.310	35.682	–1.421	36.653
–1.301	14.629	–1.136	34.512	–1.208	35.487	–1.276	35.689	–1.438	36.659
–1.284	14.634	–1.147	34.517	–1.174	35.493	–1.245	35.694	–1.438	36.664
–1.249	14.640	–1.159	34.523	–1.127	35.499	–1.404	36.462	–1.428	36.670
–1.226	14.645	–1.182	34.528	–1.087	35.504	–1.397	36.467	–1.424	36.675
–1.180	14.651	–1.224	34.533	–1.055	35.509	–1.399	36.473	–1.421	36.681
–1.141	14.656	–1.250	34.538	–1.039	35.514	–1.405	36.478	–1.415	36.686
–1.120	14.662	–1.295	34.543	–1.039	35.519	–1.397	36.484	–1.391	36.695
–1.109	14.667	–1.332	34.549	–1.037	35.525	–1.392	36.489	–1.378	36.700
–1.115	14.673	–1.353	34.554	–1.038	35.531	–1.372	36.494	–1.353	36.706
–1.106	14.678	–1.375	34.559	–1.044	35.536	–1.352	36.500	–1.318	36.711
–1.112	14.683	–1.378	34.564	–1.046	35.541	–1.330	36.505		
–1.114	14.689	–1.393	34.569	–1.057	35.546	–1.319	36.511		
–1.110	14.694	–1.408	34.575	–1.074	35.551	–1.280	36.516		

Table 2. Information on the stars used in this study.

Star	Name	R.A. (2000) h m s	Dec. (2000) ° ′ ″	V	J–K	B–V
V	V1695 Aql GSC 5149-2845 BD–03 4659	19 38 22.3027	–03 32 37.461[1]	10.92[1]	0.40	0.72 ± 0.08[1]
C	GSC 5149-2931	19 38 23.9189	–03 35 56.965[1]	11.04	—	—
K (Check)	3UC174-2249292	19 38 22.5783	–03 28 3.356[3]	12.25	0.30	—

[1] *Høg, E., et al. 2000.*

be steeper than that left as it is in Figure 12 of their paper, Molnar *et al.* 2017). So while the period is decreasing, it is not exponentially decaying at this time. If this phenomenon were present, it would lead to a rapid coalescence.

The extreme mass ratio binary has an inclination of 86°, which yields the rather long-duration total eclipse. The W UMa binary is of W-type (the less massive component is slightly hotter). This is unusual for deep contact binaries. Two cool spots were needed in the WD solution.

This initial study of V1695 Aql lays the groundwork for future work. More eclipse timings are needed to make a definitive study of its orbital evolution. We plan future follow-up observations. Of course, radial velocity curves should be obtained to determine its absolute physical character (masses in kg, radii in km, etc.).

Table 3. V1695 Aql period study.

	Epoch 2400000+	Cycles	Linear Residuals	Quadratic Residuals	Reference
1	51275.0350	–15409.5	–0.0366	–0.0024	Paschke 1994, 2002
2	52433.6990	–12603.0	0.0210	0.0163	Paschke 1994, 2002
3	52522.4400	–12388.0	0.0036	–0.0035	Berhard *et al.* 2002
4	52522.4432	–12388.0	0.0068	–0.0003	Pejcha 2005
5	52576.3098	–12257.5	–0.0008	–0.0093	Pejcha 2005
6	55405.0525	–5405.5	0.0331	–0.0014	Kazuo O–C Gateway
7	57614.6837	–53.0	–0.0064	0.0024	This Paper
8	57634.4925	–5.0	–0.0134	–0.0039	This Paper
9	57636.5626	0.0	–0.0074	0.0021	This Paper

Table 4. V1695 Aql light curve characteristics.

Filter	*Phase*	*Magnitude Max. I*	*Phase*	*Magnitude Max. II*
	0.25		0.75	
B		–1.408 ± 0.019		–1.406 ± 0.010
V		–1.408 ± 0.016		–1.431 ± 0.005
R_c		–1.386 ± 0.015		–1.401 ± 0.007
I_c		–1.406 ± 0.017		–1.432 ± 0.005

Filter	*Phase*	*Magnitude Min. II*	*Phase*	*Magnitude Min. I*
	0.0		0.5	
B		–0.993 ± 0.002		–1.077 ± 0.014
V		–1.040 ± 0.004		–1.108 ± 0.013
R_c		–0.993 ± 0.004		–1.078 ± 0.015
I_c		–1.040 ± 0.003		–1.108 ± 0.013

Filter	*Min. I – Max. I*	*Min. I – Min. II*
B	0.415 ± 0.021	0.084 ± 0.016
V	0.368 ± 0.020	0.068 ± 0.016
R_c	0.393 ± 0.019	0.085 ± 0.018
I_c	0.366 ± 0.020	0.068 ± 0.016

Filter	*Max. I – Max. II*	*Filter*	*Min. II – Max. I*
B	–0.002 ± 0.030	B	0.331 ± 0.033
V	0.023 ± 0.021	V	0.300 ± 0.028
R_c	0.015 ± 0.022	R_c	0.308 ± 0.030
I_c	0.026 ± 0.022	I_c	0.298 ± 0.029

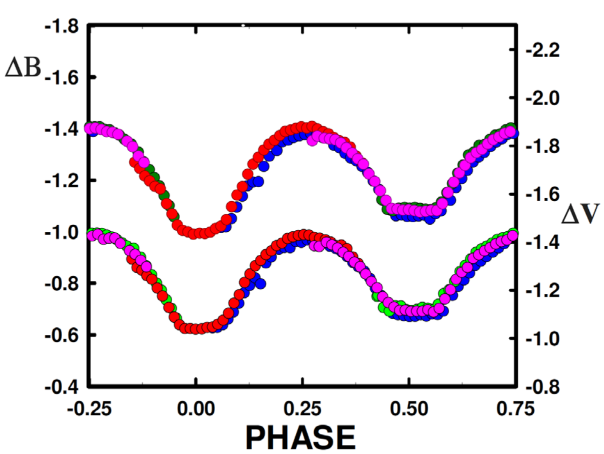

Figure 6. Each night's observations in B and V are plotted to show night to night variations in observations. Blue = night 1, Green = night 2, Red = night 3, Pink = night 4.

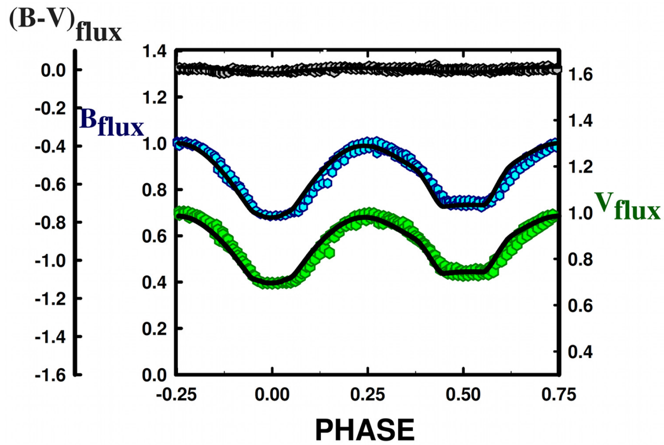

Figure 7a. V1695 Aql B, V normalized fluxes overlaid by our solution of V1695 Aql.

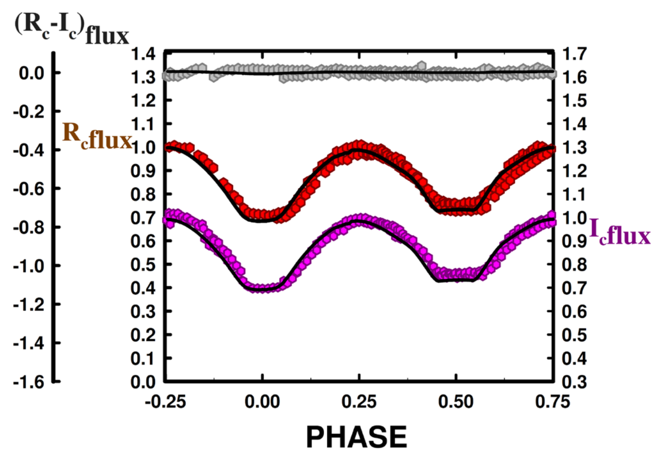

Figure 7b. V1695 Aql R_c, I_c normalized fluxes overlaid by our solution of V1695 Aql.

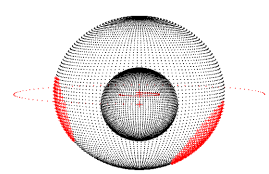

Figure 8a. V1695 Aql, geometrical representation at phase 0.00.

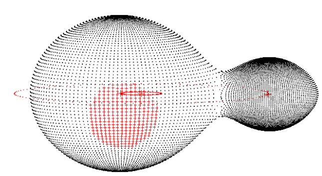

Figure 8b. V1695 Aql, geometrical representation at phase 0.25.

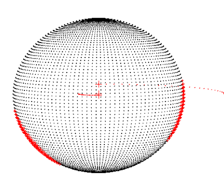

Figure 8c. V1695 Aql, geometrical representation at phase 0.50.

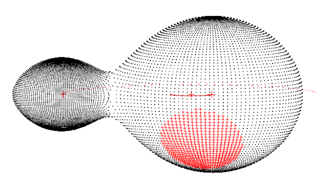

Figure 8d. V1695 Aql, geometrical representation at phase 0.75.

Table 5. Synthetic curve solution for V1695 Aql. Terms with errors are iterated values.

Parameter	*Value*
λ_B, λ_V, λ_{Rc}, λ_{Ic} (nm)	440, 550, 640, 790
$x_{bol1,2}$, $y_{bol1,2}$	0.649, 0.649, 0.193, 0.193
$x_{1Ic,2Ic}I$, $y_{1Ic,2Ic}$	0.623, 0.623, 0.230, 0.230
$x_{1Rc,2Rc}$, $y_{1Rc,2Rc}$	0.708, 0.708, 0.229, 0.229
$x_{1V,2V}$, $y_{1V,2V}$	0.778, 0.778, 0.108, 0.108
$x_{1B,2B}$, $y_{1B,2B}$	0.847, 0.847 –0.018, –0.018
g_1 , g_2	0.32
A_1 , A_2	0.5
Inclination (°)	85.6 ± 0.2
T_1, T_2 (K)	5500, 5649 ± 3
Ω_1, Ω_2	2.049 ± 0.001
$q(m_2 / m_1)$	0.1622 ± 0.0002
Fill–outs: $F_1 = F_2$	83% ± 1%
$L_1 / (L_1 + L_2)_{Ic}$	0.805 ± 0.001
$L_1 / (L_1 + L_2)_{Rc}$	0.803 ± 0.002
$L_1 / (L_1 + L_2)_V$	0.800 ± 0.001
$L_1 / (L_1 + L_2)_B$	0.792 ± 0.001
r_1, r_2 (pole)	0.525 ± 0.002, 0.246 ± 0.003
r_1, r_2 (side)	0.586 ± 0.003, 0.260 ± 0.004
r_1, r_2 (back)	0.613 ± 0.003, 0.340 ± 0.019
Spot 1	*Star 1*
Colatitude	125 ± 1
Longitude	80.6 ± 0.4
Spot radius	29.5 ± 0.1
T–Factor	0.812 ± 0.003
Spot 2	*Star 1*
Colatitude	102.2 ± 0.4
Longitude	275.4 ± 0.3
Spot radius	23.9 ± 0.01
T–Factor	0.803 ± 0.003
Pshift	0.0
JD_0 (days)	2457634.7038 ± 0.0003
Period (days)	0.412755 ± 0.000006
$\Sigma(res)^2$	0.1468

Table 6. Unspotted synthetic curve solution for V1695 Aql. Terms with errors are iterated values. The values not listed are identical as those in Table 4.

Parameter	*Value*
Inclination (°)	87.1 ± 0.5
T_1, T_2 (K)	5500, 5252 ± 4
Ω_1, Ω_2	2.114 ± 0.002
$q(m_2 / m_1)$	0.1684 ± 0.0004
Fill–outs: $F_1 = F_2$	34.8 ± 0.2%,
$L_1 / (L_1 + L_2)_I$	0.849 ± 0.010
$L_1 / (L_1 + L_2)_R$	0.852 ± 0.015
$L_1 / (L_1 + L_2)_V$	0.856 ± 0.010
$L_1 / (L_1 + L_2)_B$	0.866 ± 0.011
r_1, r_2 (pole)	0.509 ± 0.002, 0.232 ± 0.003
r_1, r_2 (side)	0.561 ± 0.003, 0.243 ± 0.003
r_1, r_2 (back)	0.585 ± 0.004, 0.287 ± 0.008
$\Sigma(res)^2$	0.1932

Table 7. Comparison of KIC 9832227 to V1685 Aql.

Star	*q*	T_1	T_2	*P*	$\dot{P}$
KIC 9832227	0.227957	5800 K	5920 K	0.4579615 d	2.0×10^{-6}
V1685 Aql	0.1622	5500 K	5649 K	0.4128296 d	1.7×10^{-6}

9. Acknowledgements

We thank the Southeastern Association for Research in Astronomy for providing observing time, as well as the Emmanuel College Natural Sciences Department for its continued support of student research projects. Student researcher Christopher R. Gray would also like to personally thank Dr. Ron Samec for his mentorship and providing the opportunity to work on the project. Finally, Gray would like to also thank Dr. Brian Peek for his leadership in overseeing the 2016–2017 Research Symposium at Emmanuel College.

References

Bernhard, K., Kiyota, S., and Pejcha, O. 2002, *Inf. Bull. Var. Stars*, No. 5318, 1.
Bradstreet, D. H., and Steelman, D. P., 2002, *Bull. Amer. Astron. Assoc.*, **34**, 1224.
Gazeas, K., and Stępień, K. 2008, *Mon. Not. Roy. Astron. Soc.*, **390**, 1577.
Hoffman, D. I., Harrison, T. E., and McNamara, B. J. 2009, *Astron. J.*, **138**, 466.
Høg, E., *et al.* 2000, *Astron. Astrophys.*, **355**, L27.
Kazarovets, E. V., Samus, N. N., Durlevich, O. V., Kireeva, N. N, and Pastukhova, E. N. 2006, *Inf. Bull. Var. Stars*, No. 5721, 1.
Kreiner, J. M. 2004, *Acta Astron.*, **54**, 207.
Kwee, K. K., and Van Woerden, H. 1956, *Bull. Astron. Inst. Netherlands*, **12**, 327.
Molnar, L. A. 2017, private communication (June 26).
Molnar, L. A., *et al.* 2017, *Astrophys. J.*, **840**, 1.
Nelson, R. 2016, Nelson Database of Times of Minima (https://www.aavso.org/bob-nelsons-o-c-files).
Paschke, A. 1994, observations of V1695 Aql in O–C Gateway (http://var2.astro.cz/ocgate/).
Paschke, A. 2002, observations of V1695 Aql in O–C Gateway (http://var2.astro.cz/ocgate/).
Pejcha, O. 2005, *Inf. Bull. Var. Stars*, No. 5645, 1.
Rasio, F. A. 1995, *Astrophys. J., Lett.*, **444**, L41.
Szczygiel, D. M., Socrates, A., Paczynski, B., Pojmanski, G., and Pilecki, B. 2008, *Acta Astron.*, **58**, 405.
Van Hamme, W., and Wilson, R. E. 1998, *Bull. Amer. Astron. Soc.*, **30**, 1402.
Van Hamme, W., and Wilson, R. E. 2003, in *GAIA Spectroscopy: Science and Technology*, ed. U. Munari, ASP Conf. Ser. 298, Astronomical Society of the Pacific, San Francisco, 323.
Wilson, R. E. 1990, *Astrophys. J.*, **356**, 613 .
Wilson, R. E. 1994, *Publ. Astron. Soc. Pacific*, **106**, 921 .
Wilson, R. E. 2001, *Inf. Bull. Var. Stars*, No. 5076, 1.
Wilson, R. E. 2004, *New Astron. Rev.*, **48**, 695 .
Wilson, R. E., and Devinney, E. J. 1971, *Astrophys. J.*, **166**, 605.